Interface formation and electronic structure of α-sexithiophene on ZnO

S. Blumstengel,[1,a)] N. Koch,[1] S. Sadofev,[1] P. Schäfer,[1] H. Glowatzki,[1] R. L. Johnson,[2] J. P. Rabe,[1] and F. Henneberger[1]
[1]*Institut für Physik, Humboldt-Universität zu Berlin, Newtonstr.15, 12489 Berlin, Germany*
[2]*Universität Hamburg, Institut für Experimentalphysik, 22761 Hamburg, Germany*

(Received 28 January 2008; accepted 31 March 2008; published online 12 May 2008)

Interface formation between the organic semiconductor α-sexithiophene (6T) and polar as well as nonpolar ZnO surfaces is investigated. The growth mode of the organic layer is strongly influenced by the orientation of the ZnO surface. No indication for chemisorption of 6T on ZnO is found by photoelectron spectroscopy. The energy level alignment at the 6T/ZnO interface is of type-II facilitating electron transfer from the organic to the inorganic part and hole transfer in the other direction, rendering this heterostructure interesting for photovoltaic applications. © *2008 American Institute of Physics*. [DOI: 10.1063/1.2918089]

Organic/ZnO hybrid structures currently attract much attention as they promise material properties that cannot be achieved with the individual component alone. Recently, it has been shown that efficient exciton as well as charge transfer across the organic/inorganic interface can be achieved.[1,2] Moreover, ZnO is easily nanostructured. These features predestine organic/ZnO hybrid structures for applications in light-emitting devices, photodiodes, or photovoltaic cells. The functionality of these devices depends on the interface between the two types of materials. This concerns the interfacial electronic structure as well as its morphology and crystalline quality. In this letter, we report on the interface formation of α-sexithiophene (6T) with various ZnO crystal faces. We show that by choosing proper conditions, the growth of 6T on ZnO is diffusion limited and not perturbed by surface defects or step edges resulting in crystalline layers. The molecules adsorb intact and form, regarding the energy level alignment, a type-II interface with ZnO as revealed by photoelectron spectroscopy.

To ensure the preparation of a clean well-defined interface, both ZnO as well as 6T are grown by molecular beam epitaxy/deposition under ultrahigh vacuum conditions in a DCA apparatus with interconnected growth chambers for organic and inorganic materials. ZnO crystallizes in wurtzite structure. The different crystal faces possess quite different chemical and structural properties[3] which, as we will show here, influence the growth of the molecular overlayer. To obtain epitaxial O-terminated ZnO$(000\bar{1})$, Zn-terminated ZnO(0001), and mixed-terminated ZnO$(10\bar{1}0)$ surfaces, $(000\bar{1})$, (0001), and $(10\bar{1}0)$ oriented ZnO substrates (CrysTec) were overgrown with a 50 nm thick ZnO layer, respectively. The ZnO$(000\bar{1})$ surface shows a well pronounced (3×3) reconstruction in the reflection high energy electron diffraction pattern, while (0001) possesses a weak (4×4) or (2×2) reconstruction. The ZnO$(10\bar{1}0)$ surface is unreconstructed. Atomic force microscopy (AFM) (Digital Instruments) reveals that both polar surfaces are atomically smooth with monolayer steps of a height of 2.6 Å. ZnO$(10\bar{1}0)$ shows a corrugated surface with elongated flat terraces along the (0001) direction. 6T (Aldrich, purified by sublimation before use) was deposited on epitaxial ZnO in the submonolayer up to a few layer range keeping the growth rate constant at 1 Å/min as measured with a quartz microbalance.

Representative AFM images of 6T submonolayers deposited on the three differently oriented ZnO epilayers are depicted in Fig. 1. On ZnO$(000\bar{1})$ [Fig. 1(a)], the nucleation of 6T is heterogeneous as there is more than one length scale observed. This regards the size as well as the distance between the islands. The images reveal the presence of different crystal shapes. There are flat islands whose height (~2.5 nm) corresponds to half the *a*-lattice constant of the 6T crystal[4] and which are therefore attributed to upright or nearly upright standing molecules. Moreover, there are laterally smaller but much higher (~15 nm) crystallites, some of them are needle shaped. As the growth velocity is strongly dependent on the crystallographic direction in an anisotropic crystal as 6T, the higher islands most likely have a different contact plane with the molecules oriented parallel to the substrate surface. After start of the growth, a dead time corresponding approximately to the deposition of about $\frac{1}{10}$ of a monolayer (ML) is observed in which no nucleation occurs. At this growth stage, incoming molecules become immobilized at surface defects or dangling bonds present at ZnO$(000\bar{1})$. Nucleation sets in only after passivation of these sites. These observations indicate that the nucleation is governed by surface defects resulting in a poor crystalline quality of the organic layer. The growth scenario does not qualitatively change by varying the substrate temperature T_S

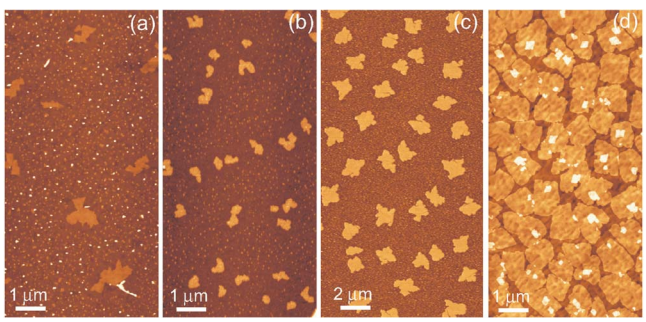

FIG. 1. (Color online) AFM images of 6T deposited on (a) ZnO$(000\bar{1})$, T_S=75 °C, (b) ZnO(0001), T_S=25 °C, and (c) T_S=100 °C, respectively and (d) ZnO$(10\bar{1}0)$, T_S=25 °C.

a)Electronic mail: sylke.blumstengel@physik.hu-berlin.de.

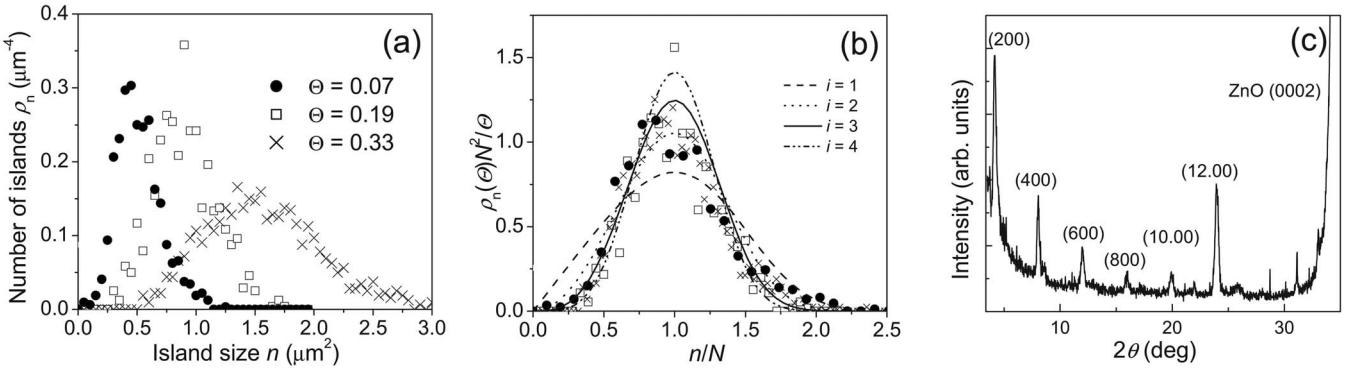

FIG. 2. (a) Size distribution of 6T islands deposited on ZnO(0001) for different coverages Θ. The substrate temperature is 100 °C. (b) Scaled island size distributions (symbols) and scaling function $f(u)$ for $i=1-4$ (lines). (c) XRD of 6T on ZnO(0001) deposited at $T_S=100$ °C.

between 25 and 120 °C. This is in contrast to the growth on ZnO(0001). At $T_S=25$ °C, island sizes and distances between the islands follow a distinct bimodal distribution. The height of the islands is constant corresponding to the length of the 6T molecule, i.e., the contact plane is the (100) plane of crystalline 6T, indicative of a weakly interacting substrate where intermolecular interactions outbalance molecule-substrate interaction.[5] Increasing T_S to 100 °C, the growth mode changes. Nucleation becomes homogenous, as seen in Fig. 1(c), and the small islands are no longer present. On ZnO(10$\bar{1}$0) [Fig. 1(d)], the nucleation is homogeneous already at $T_S=25$ °C. The islands are composed again of upright standing molecules. Pronounced step edges with a height corresponding to up to 5 ML steps (each of $h=2.81$ Å) present on this ZnO surface obviously have no effect on the growth of the organic layer. Nucleation of the 6T islands sets in immediately after the start of the deposition on both ZnO(0001) and ZnO(10$\bar{1}$0) irrespective of T_S.

The absence of an initial dead time as well as homogenous nucleation on ZnO(0001) at $T_S=100$ °C and ZnO(10$\bar{1}$0) point toward a diffusion-limited growth process.[6] The island morphology is then determined by the kinetics of the process characterized by the ratio of the diffusion constant D and the incoming flux F, $R=D/F$. A fingerprint of such growth process is that scaling laws apply for structural quantities such as the islands size distribution as a function of the coverage Θ and R. To check the hypothesis, we extracted the island size distribution of 6T deposited at $T_S=100$ °C on ZnO(0001) for different coverages [see Fig. 2(a)] from AFM images taken in the aggregation regime. The mean island area size N as well as the width of the distribution increase with Θ. In the frame of the dynamic scaling approach, the number ρ_n of islands (per unit area) of area size n can be represented by the scaling law $\rho_n=(\Theta/N^2)f(u)$, where $f(u)$ is the scaling function with $u=n/N$.[6,7] Figure 2(b) shows that the scaled island size distributions indeed transform into a single curve in excellent agreement with the above relation. The shape of the island size distribution sensitively depends on the critical nucleus. On the basis of numerical simulations, an empirical expression $f(u)=C_i u^i \exp(-ia_i u^{1/a_i})$ was proposed for the scaling function where $i+1$ is the number of molecules needed to form a stable nucleation seed.[8] C_i and a_i are constants assuring normalization of $f(u)$.[9] In Fig. 2(b), $f(u)$ is drawn for different values of i. The curve for $i=3$ fits best the experimental data. That means that the smallest stable nucleus is comprised of four 6T molecules. A similar number was found for pentacene deposited on oxidized silicon.[10] The good quantitative agreement between the experimental data and the scaling function confirms that the growth of 6T on ZnO(0001) [and likely on ZnO(10$\bar{1}$0) as well] in the ML regime is diffusion limited and not perturbed by the presence of surface defects, dangling bonds, or step edges. Continuing the deposition of 6T to obtain films several tenths of nm thick, the growth direction is retained with the 6T(100) plane parallel to the ZnO(0001) surface. This is evidenced by the x-ray diffractogram (XRD) of a 25 nm thick 6T film on ZnO(0001) [Fig. 2(c)] collected with a Philips PW28 powder diffractometer using $\theta/2\theta$ scanning with Cu $K\alpha$ radiation and an analyzer crystal. It shows the well pronounced (200), (400), (600), (800), (10.00), and (12.00) reflections of the low temperature phase of crystalline 6T.[4]

The bonding state of the 6T/ZnO(0001) and 6T/ZnO(000$\bar{1}$) interfaces was probed by x-ray photoelectron spectroscopy (XPS). Photoelectrons were excited with radiation from a nonmonochromated Al anode (Al $K\alpha$: 1486.85 eV), and detected by a hemispherical analyzer (Specs) with a resolution of about 0.8 eV. In Fig. 3, the evolution of the O 1s as well as the S 2p spectra of the 6T/ZnO(000$\bar{1}$) interface with increasing thickness d_{6T} of the organic layer is depicted. The pristine ZnO surface shows a peak at 530.7 eV indicative of O–Zn bonding. A feature at

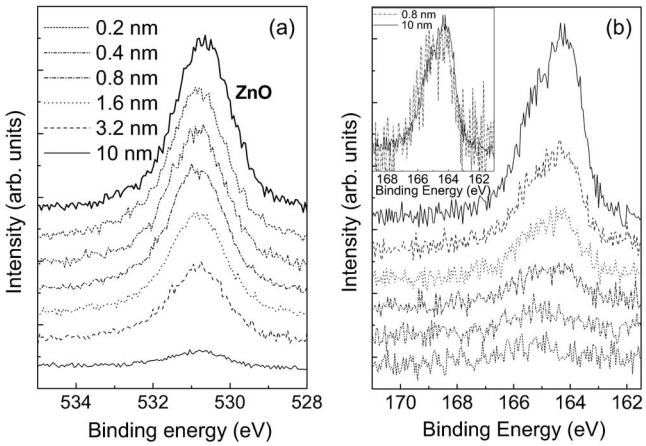

FIG. 3. Dependence of the ZnO O 1s (a) and 6T S 2p (b) core level spectra on d_{6T} for the 6T/ZnO(000$\bar{1}$) interface. To allow better comparison, the normalized 6T S 2p spectra for 0.8 and 10 nm coverage are depicted in the inset.

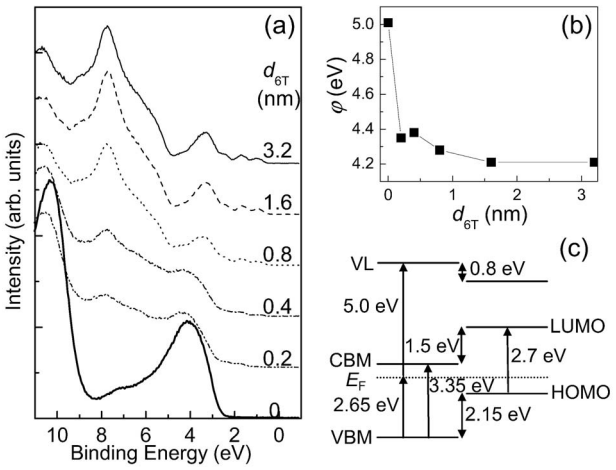

FIG. 4. (a) Dependence of the valence region UPS spectra and (b) work function of 6T/ZnO(000$\bar{1}$) on d_{6T}. The photon energy is 22 eV. (c) Energy level diagram of the interface. The exciton binding energy of ZnO is 60 meV and of 6T it is assumed to be 0.4 eV (Ref. 15). VL denotes vacuum level.

532.9 eV characteristic for O–OH bonding is not detected. The intensity of the peak decreases with increasing 6T coverage. The substrate core levels O 1*s* [Fig. 3(a)] and Zn 2*p* (not shown) experience a rigid shift by 0.1 eV toward higher binding energies upon deposition of 6T most likely caused by a change in band bending at the ZnO(000$\bar{1}$) surface. The binding energies of the S 2*p* [Fig. 3(b)] and C 1*s* (not shown) states decrease by ~0.5 eV with increasing 6T thickness within the first few angstroms and remain constant for larger film thicknesses. This shift is due to more efficient photohole final state screening for larger 6T islands as more polarizable matter is provided by neighboring molecules.[11] At high coverage, the spin orbit split S $2p_{3/2}$ (164.15 eV) and S $2p_{1/2}$ (165.35 eV) contributions to the overall S 2*p* peak can be clearly discerned. As the shape of all spectra remains independent of d_{6T} (demonstrated in the inset in Fig. 3(b), with the spectra for 0.8 and 10 nm scaled to the same intensity), chemical bond formation at the 6T/ZnO(000$\bar{1}$) can be ruled out. The spectra of the 6T/ZnO(0001) interface show a similar behavior and are therefore not depicted, signifying that the molecules are physisorbed on these semiconductor surfaces. This is in marked contrast to other semiconductor surfaces like Si(100) on which even fragmentation of 6T was observed.[12]

Ultraviolet photoelectron spectroscopy (UPS) was employed to measure the band offsets between the highest occupied molecular orbital (HOMO) of 6T and the valence band maximum (VBM) of ZnO $\Delta E_{VBM/HOMO}=E_{VBM}-E_{HOMO}$. The measurements were performed at the FLIPPER II station at HASYLAB (Hamburg, Germany), for experimental details see Ref. 13. The valence UPS spectrum of ZnO(000$\bar{1}$) [bottom curve in Fig. 4(a)] shows a peak at 4.2 eV which is related to the O 2*p* orbital.[14] Upon deposition of 6T, the photoemission intensity from ZnO is attenuated and well-resolved features due to 6T molecular levels appear. At intermediate 6T thicknesses, the spectra are superpositions of the ZnO and molecule spectra. No changes in the electronic structure can be detected in agreement with XPS. The energy difference between the low binding energy onset of the top and bottom spectra of Fig. 4(a) yield the energy offset $\Delta E_{VBM/HOMO}=-2.15$ eV. Note that the offset may be 0.1 eV larger due to the adsorbate-induced change of the ZnO surface band bending (see discussion of XPS spectra above). From the shift of the secondary electron cutoff in Fig. 4(b) a change of the work function φ from 5.0 to 4.2 eV is deduced revealing a modification of the surface dipole and/or the electron-density distribution on the ZnO(000$\bar{1}$) surface. The offset between the ZnO conduction band minimum (CBM) and the 6T lowest unoccupied molecular orbital (LUMO) $\Delta E_{CBM/LUMO}=E_{CBM}-E_{LUMO}=-1.5$ eV is obtained by adding to E_{VBM} and E_{HOMO} the optical band gaps, obtained from absorption measurements, and the exciton binding energies of the respective component. The resultant energy schematics are represented in Fig. 4(c), 6T/ZnO(000$\bar{1}$) forms a type-II heterointerface with regard to the energy level alignment facilitating electron transfer from the 6T to ZnO and hole transfer in the other direction.

To conclude, the results imply that 6T/ZnO hybrid structures are promising for photovoltaic applications. The band offsets at the type-II interface are sufficiently large to allow for efficient charge separation. Choosing the proper ZnO crystal face, the assembly of the molecules is not influenced by step edges, dangling bonds or surface defects facilitating diffusion-limited growth resulting in crystalline layers with the domain size tunable by the substrate temperature. Crystallinity of the organic materials is a prerequisite to achieve large exciton diffusion lengths required to transport a large fraction of photogenerated excitons to the heterointerface. By using nanostructured ZnO, for instance in the form of nanorods, the geometry can be optimized in such a manner to balance absorption and exciton diffusion to the interface.

Financial support of the Deutsche Forschungsgemeinschaft within the frame of Sfb 448 is acknowledged.

[1] S. Blumstengel, S. Sadofev, C. Xu, J. Puls, and F. Henneberger, Phys. Rev. Lett. **97**, 237401 (2006).
[2] A. Furube, M. Murai, S. Watanabe, K. Hara, R. Katoh, and M. Tachiya, J. Photochem. Photobiol., A **182**, 273 (2006).
[3] C. Wöll, Prog. Surf. Sci. **82**, 55 (2007).
[4] G. Horowitz, B. Bachet, A. Yassar, P. Lang, F. Demanze, J. L. Fave, and F. Garnier, Chem. Mater. **7**, 1337 (1995).
[5] P. Lang, M. ElArdhaoui, J. C. Wittmann, J. P. Dallas, G. Horowitz, B. Lotz, F. Garnier, and C. Straupe, Synth. Met. **84**, 605 (1997).
[6] T. Vicsek, *Fractal Growth Phenomena* (World Scientific, Singapore, 1992).
[7] M. C. Bartelt and J. W. Evans, Phys. Rev. B **46**, 12675 (1992).
[8] J. A. Stroscio and D. T. Pierce, Phys. Rev. B **49**, 8522 (1994).
[9] J. G. Amar and F. Family, Phys. Rev. Lett. **74**, 2066 (1995).
[10] R. Ruiz, B. Nickel, N. Koch, L. C. Feldman, R. F. Haglund, A. Kahn, F. Family, and G. Scoles, Phys. Rev. Lett. **91**, 136102 (2003).
[11] I. G. Hill, A. J. Mäkinen, and Z. H. Kafafi, J. Appl. Phys. **88**, 889 (2000).
[12] R. Lin, M. Galili, U. J. Quaade, M. Brandbyge, T. Bjørnholm, A. Degli Esposti, and F. Biscarini, J. Chem. Phys. **117**, 321 (2002).
[13] S. Blumstengel, N. Koch, S. Duhm, H. Glowatzky, R. L. Johnson, C. Xu, A. Yassar, J. P. Rabe, and F. Henneberger, Phys. Rev. B **73**, 165323 (2006).
[14] R. T. Girard, O. Tjernberg, G. Chiaia, S. Soderholm, U. O. Karlsson, C. Wigren, H. Nylen, and I. Lindau, Surf. Sci. **373**, 409 (1997).
[15] I. G. Hill, A. Kahn, Z. G. Soos, and R. A. Pascal, Chem. Phys. Lett. **327**, 181 (2000).